Amplification of Femtosecond Laser Filaments in Ti:Sapphire

J. Philip,[1] C. D'Amico,[1] G. Chériaux,[1] A. Couairon,[2] B. Prade,[1] and A. Mysyrowicz[1]

[1]*Laboratoire d'Optique Appliquée, CNRS UMR 7639, Ecole Nationale Supérieure des Techniques Avancées, Ecole Polytechnique, F-91761 Palaiseau, France*

[2]*Centre de Physique Théorique, CNRS UMR 7644, École Polytechnique, F-91128 Palaiseau, France*

(Received 21 December 2004; revised manuscript received 22 April 2005; published 12 October 2005)

Femtosecond laser filamentation is studied in a broadband amplifying medium, sapphire doped with electronically excited Ti ions. Evidence for fluence amplification of self-guided pulses, increase of filamentation length, as well as a lowering of the input laser power necessary for filamentation is reported.

DOI: 10.1103/PhysRevLett.95.163901 PACS numbers: 42.25.Bs, 42.65.Jx, 42.65.Re, 42.65.Sf

Much attention has been given in the last few years to the propagation of ultrashort laser pulses through continuous transparent media. With short pulses (pulse duration $<10^{-12}$ s), high peak intensities are achieved with modest energy per pulse. As a consequence, the dielectric medium is readily driven into a nonlinear regime. The nonlinear polarization in turn induces significant changes in the pulse characteristics. This can lead to spectacular new effects. For instance, several groups have reported the occurrence of femtosecond filamentation [1–9]. In this process, an intense ultrashort laser pulse self-organizes into a contracted beam, 10–100 μm in diameter, fed by a surrounding laser energy reservoir. It carries a peak intensity higher than the initial one over distances which can reach several km in air, well beyond the Rayleigh range. Filamentation is accompanied by a temporal self-contraction of the pulse, an effect occurring even if the pulse propagates in a region of normal dispersion, where pulse lengthening is expected in a linear regime. Self-contraction of laser pulses by filamentation down to nearly a single-cycle pulse has been recently reported [10].

The principal effects responsible for filamentation are well recognized. Filamentation results predominantly from a dynamic competition between the optical Kerr effect and multiphoton ionization, even if other effects, such as pulse self-steepening, spectral broadening by self-phase modulation, and beam diffraction take part in the pulse reshaping. The optical Kerr effect is responsible for self-focusing, a process initiating beam collapse if the input laser pulse power exceeds a critical value $P_{\mathrm{cr}}^{\mathrm{th}} = \lambda^2/2\pi n_0 n_2$, where λ, n_0, and n_2 denote the laser wavelength, the linear index, and the nonlinear index coefficient, respectively. Multiphoton ionization sets in once the beam intensity reaches a sufficiently high value. The multiphoton ionization rate scales as I^n, where I is the laser intensity and n, the number of photons simultaneously absorbed, is typically greater than 5 for infrared wavelengths. The generated electron density has therefore a thresholdlike response, which saturates self-focusing locally and limits the peak intensity inside the filament by defocusing the beam. The dynamic interplay between self-focusing and ionization is therefore a highly dynamic process, with recurrent, aperiodic strings or spikes of ionization surging whenever the beam starts collapsing again [11]. Energy losses during filamentation are minimized because (a) the intensity is always maintained at the verge or below the value corresponding to ionization threshold via this clamping mechanism and (b) the short pulse duration prevents significant pulse attenuation through its interaction with the generated plasma (via inverse Brehmsstrahlung). Femtosecond filamentation has been observed in air and other gases, in solids, and in liquids [1–16]. Except for scaling factors, the physics is basically the same in all media, although the relative importance of the various physical effects may differ from one medium to another [17]. Experimental results are well reproduced by numerical simulations which resolve a 3D nonlinear Schrödinger equation for the evolution of the laser field envelope [16,18]. Typical values for the critical power are in the GW range for gas and the MW range in solids such as fused silica or sapphire [19]. Both in solids and gases the maximum intensity inside the filament is clamped to a value around a few 10^{13} W cm^{-2} [20].

The purpose of this Letter is to describe a study of filamentation in an amplifying medium. We show, for the first time, that it is possible to induce the formation of a filament even if the incident pulse power is below threshold. One can also, when using an incident pulse with power above critical, increase the length of a filament and amplify its fluence. More generally, by decoupling the formation of a filament from its subsequent amplification, one is able to maintain and extend the range of a *single* filament. This has to be contrasted with the approach consisting in increasing the pulse power before filamentation. In the latter case, multifilamentation unavoidably occurs because initial irregularities of the beam intensity profile are reinforced, leading to an erratic pattern, unless provision is taken to organize it [18,21–23].

We have performed the experiments in a 1.2 cm long single crystal of sapphire doped with Ti^{3+} ions. This offers a convenient laboratory size system with a very large amplifying bandwidth. The experimental setup is shown in Fig. 1. The output of a Ti:sapphire laser (pulse duration

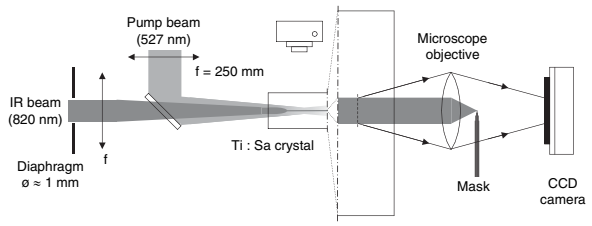

FIG. 1. Experimental setup (see text). The right part of the figure magnifies the Schlieren imaging technique.

50 fs or 80 fs) centered around 820 nm at 1 kHz repetition rate is focused with a lens on the entrance plane of the sample held at room temperature. The experiments have been performed with several convergent beams, showing essentially similar results. The maximum energy per pulse of the laser is 1 mJ but only pulses with a few μJ are used here since we concentrate on the regime $P \sim P_{\rm cr}$, where $P_{\rm cr}$ denotes the power required for the onset of filamentation within our 1.2 cm long sample. $P_{\rm cr}$ is larger than the theoretical $P_{\rm cr}^{\rm th} = 1.9$ MW, which is calculated under the assumption of a CW laser and a Gaussian beam in a nondispersive medium of infinite length. For $P_{\rm cr}^{\rm th} < P < P_{\rm cr}$, the self-focusing length exceeds the size of the sample and no beam collapse can be observed. The beam profile at different depths in the crystal is measured by imaging it with a microscope objective on a high contrast CCD camera (1024 gray levels of resolution). We use a ''Schlieren'' imaging technique which images the conical emission of the filament at various depths (as shown in the right part of Fig. 1.) The Ti ions of the sample can be easily brought in the excited metastable state ^2E_g by pumping the crystal longitudinally with a ns pulse at 527 nm, obtained by harmonic generation of a Nd:YLF laser. 70% of the pumping beam is absorbed, giving a fairly homogeneous gain along the propagation axis. The volume of the gain region is approximately a cylinder, 500 μm in diameter, larger than the filament. The green pumping pulse is launched $\sim$1 μs before the passage of the IR pulse.

We first consider filamentation in the unpumped crystal. Figure 2 shows a side view photograph of a filament traversing the sample when a 4 μJ, 50 fs pulse is focused with a $f = 20$ cm lens onto the entrance face of the sample. The image corresponds to the luminescence of the crystal excited by the pulse and reflects the intensity pattern of the propagating pulse. Instead of diffracting according to the law of linear optics, the beam takes the shape of a narrow core $\sim$10 μm in diameter. This core is maintained over a distance of about 1 cm, corresponding to the length of the crystal. Furthermore, one distinguishes several intensity maxima along the propagation axis. This provides a striking illustration of the expected recurrent cycles of refocusing yielding secondary collapses, as first pointed out in Refs. [11,20,24,25]. The size of the filament core is determined from the photograph and also by recording the beam intensity profile at the exit face of the crystal as shown in Fig. 3(b). For comparison, the beam profile for $P < P_{\rm cr}$ is also shown [see Fig. 3(a)]. One clearly notices the shrinkage of the beam waist to a radius of about 10 μm if $P > P_{\rm cr}$. By further increasing P, one eventually observes the formation of two or more filaments as shown in Fig. 3(c). We note that no appreciable damage of the crystal is observed under such conditions.

This behavior is well reproduced by numerical simulations, as shown in Fig. 4. They were obtained by solving a three-dimensional propagation equation for the laser field coupled to an evolution equation for the density of electron-hole pairs generated in the wake of the pulse via multiphoton absorption. The physical effects taken into account include diffraction, self-focusing, and self-phase modulation, multiphoton absorption and ionization, group velocity dispersion, pulse self-steepening, plasma absorption, and avalanche ionization. A detailed description of the physical model can be found in [16,18]. Here, the propagation of a 50 fs, 3.7 μJ laser pulse was computed in Ti:sapphire with $n_2 = 3 \times 10^{-16}$ cm^2 W^{-1} [19]. Multiphoton ionization is computed according to Keldysh's formulation [26] with a gap of 7.3 eV and an effective mass for electron-hole pairs $m^* = 0.35 m_e$. Figure 4(a)

FIG. 2. Side view photograph of a filament generated in an unpumped Ti:sapphire crystal with a pulse duration of 50 fs, a focusing lens of 20 cm, and an incident energy of 3.7 mJ. The converging laser beam is incident on the left side. A filament with $\sim$10 μm diameter is formed over the crystal length, displaying several secondary intensity maxima.

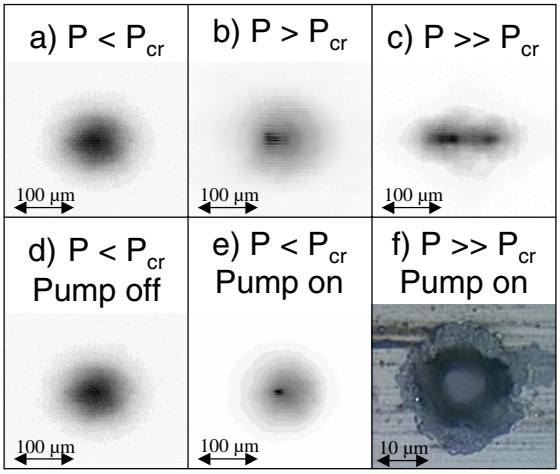

FIG. 3 (color online). Beam profile measured at the exit face of the crystal for several conditions. (a) $P < P_{\rm cr}$, unpumped crystal; (b) $E = 12$ μJ, unpumped crystal; (c) $E = 47$ μJ, unpumped crystal; (d) same as (a), (e) $E = 3.6$ μJ, pumped crystal; (f) image of the damage seen through a microscope (note the change of scale). In all cases, the pulse duration was 80 fs and the focus length of the lens was 8 cm.

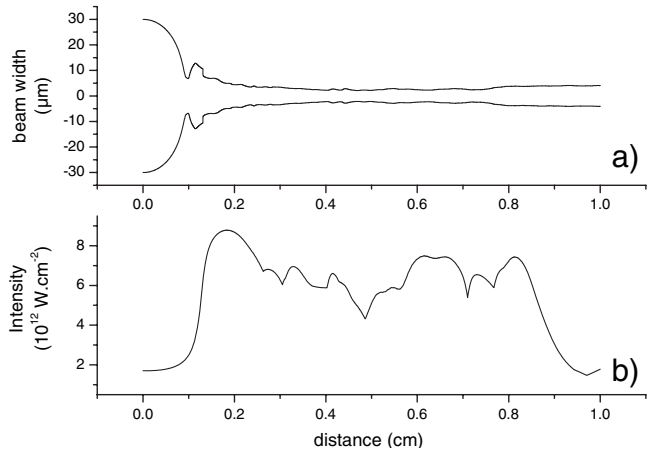

FIG. 4. (a) Computed beam width (FWHM of fluence distribution) for input power $P = 70$ MW and an input beam diameter of 60 μm. The incident beam is focussed on the entrance plane with a flat phase. This corresponds to the experimental conditions of Fig. 2. (b) Computed on-axis intensity of the pulse in the filament. Note the appearance of several intensity peaks at $\sim$2, 6, and 8 mm.

shows the beam width (FWHM of the fluence) and the on-axis intensity [Fig. 4(b)] calculated as a function of the propagation distance. A narrow light string is formed with a nearly constant diameter of about 10 microns over 1 cm. In agreement with experimental observation, the pulse refocuses several times during the 1 cm path, leading to multiple refocusing peaks with intensities reaching 8×10^{12} W cm^{-2}. About 25% of the input energy is lost via multiphoton and plasma absorption. The computed fluence in this case does not exceed 0.5 J cm^{-2}, below the characteristic damage fluence of transparent optical materials [27].

We have modified our code to include the amplification process. It is treated as an effective 4 level system, with a resonance absorption cross section $\sigma = 6.8 \times 10^{-20}$ cm^2, following typical parameters obtained from the literature [28] and a total density of Ti atoms of 5×10^{19} cm^{-3}. The modeling of the volume excited by the pumping green laser corresponds to the experimental conditions. However, for simplicity, we assume a flat spectral gain bandwidth. This assumption is reasonable for single pass amplification. Several new features are predicted in the presence of gain. Filamentation is expected to occur even if $P < P_{cr}$, a feature which can be easily understood by noting that the pulse power in the initial pure Kerr region can be now amplified until it satisfies the conditions for beam collapse inside the sample. If the incident pulse has power $P > P_{cr}$, the filament length inside the crystal should increase due to the shift of the nonlinear focus towards the entrance face of the sample. The filament should persist as long as it propagates in an excited medium.

Experimental results obtained with an amplifying crystal show several predicted effects, such as an extension of the filament length inside the crystal, an increase of its fluence, and the onset of filamentation at subthreshold power level. Figures 3(d) and 3(e) show a comparison of the beam profile measured at the exit face of the crystal, with and without population inversion. The incident energy was 3.6 μJ for the 80 fs pulse at 820 nm and 1.6 mJ for the 200 ns pulse at 527 nm. With the green pump on, a clean intense 10 μm spot is apparent. By contrast, with the green pump off, a larger beam waist is observed at the same distance. In Figs. 5(a), 5(c), and 5(d), we show the filament diameter extracted from sequences of schlieren images recorded at different depths inside the crystal. As can be seen in trace (a) of Fig. 5, pumping of the crystal with green light induces a beam collapse at $z \leq 7$ mm, corresponding to the onset of filamentation. These results are well reproduced numerically, as shown in Fig. 5(a) by continuous lines. Figure 5(b) shows the computed intensity inside the filament core with and without pumping. When $P > P_{cr}$, an extension of the filament range is also seen [as shown experimentally in Figs. 5(c) and 5(d)] due to a shift of the beginning of the filament towards the entrance face of the sample. Finally, evidence for an increase of the filament fluence is obtained by measuring the output fluence with a power meter. An amplification of the total transmitted energy by a factor up to 3 in a single pass is

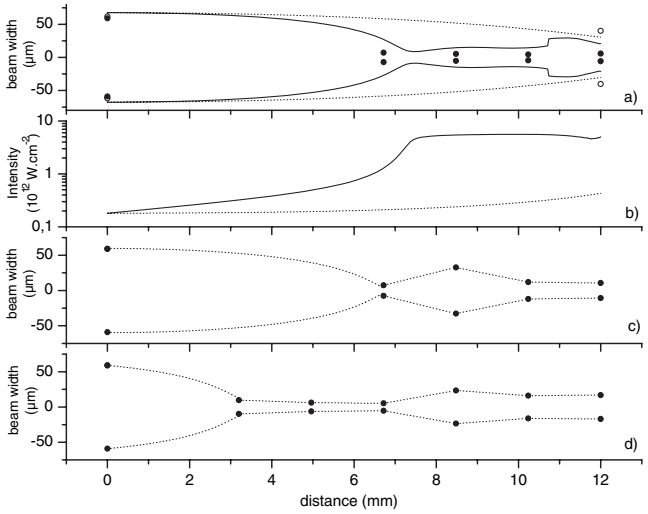

FIG. 5. (a) Beam spatial profile as a function of propagation distance inside the crystal. Circles: experimental data with pump at 527 nm off; black dots: experimental data with pump on; dotted line: simulation with pump off; solid line: simulation with pump on. The incident pulse energy is 3.6 μJ. (b) Computed intensity as a function of propagation distance. Dotted line: with pump off; solid line: with pump on. The pulse parameters correspond to Fig. 5(a). (c) Beam spatial profile measured at different depths in the crystal with pump off. The incident pulse energy is 12 μJ. Black dots: experimental data; dotted line: guide fore the eyes. (d) Beam spatial profile measured at different depths in the crystal with pump. The incident pulse energy is 12 μJ. Black dots: experimental data; dotted line: guide for the eyes. In all cases, the pulse duration was 80 fs and the focus length of the lens was 8 cm.

detected. We also notice that irreversible damage is done to the sample. The damage spot, which occurs near the output face of the crystal, takes the form of a circular spot ~ 10 μm in diameter [as shown in Fig. 3(f)], which corresponds to the size of filament core. Thus, the filament core fluence has indeed been amplified beyond the threshold for damage of doped sapphire $F \sim 0.5$ J cm^{-2} without breaking up in two or more filaments. This is not the case in an unpumped crystal.

Filament amplification is not restricted to the case considered here. It should also apply to other media such as dyes in solution, for which the damage issue is less constraining. Filament amplification may find applications in several areas. For instance, by initiating beam collapse in the form of a Townes mode over a reduced distance, it could test in a large class of transparent media the law of universal beam collapse discussed recently by Moll, Gaeta, and Fibich [29]. Filament amplification can also provide a venue to form well controlled, intense ultrashort light bullets [30]. As already mentioned, filamentation in gases is accompanied by an important pulse self-compression. The same effect can be expected in solids and liquids. By upscaling the fluence of the compressed pulse while maintaining a single filament, one should obtain nearly single-cycle multiterawatt optical pulses. Such ultrashort intense pulses are a key feature for the generation of attosecond XUV pulses [31]. Well controlled, intense single filaments launched in the atmosphere can be expected to have interesting properties over long distance, such as improved aiming accuracy, since their reduced size makes them less sensitive to air turbulence. Finally, filament amplification could also be useful in situations requiring energy transfer in condensed matter over a long path, as, e.g., for the production of bulk optical devices such as buried gratings as well as for the realization of quasi-one-dimensional amplifying geometries for short-lived gain media.

This work was partially supported by US army Contract ERO No. FA 8655-04-12081.

[1] A. Braun, G. Korn, X. Liu, D. Du, J. Squier, and G. Mourou, Opt. Lett. **20**, 73 (1995).
[2] E. T. J. Nibbering, P. F. Curley, G. Grillon, B. S. Prade, M. A. Franco, F. Salin, and A. Mysyrowicz, Opt. Lett. **21**, 62 (1996).
[3] O. G. Kosareva, V. P. Kandidov, A. Brodeur, C. Y. Chien, and S. L. Chin, Opt. Lett. **22**, 1332 (1997).
[4] B. La Fontaine, F. Vidal, Z. Jiang, C. Y. Chien, D. Comtois, A. Desparois, T. W. Johnston, J.-C. Kieffer, and H. Pépin, Phys. Plasmas **6**, 1615 (1999).
[5] D. Mikalauskas, A. Dubietis, and R. Danielus, Appl. Phys. B **75**, 899 (2002).
[6] J. Schwarz, P. Rambo, J.-C. Diels, M. Kolesik, E. M. Wright, and J. V. Moloney, Opt. Commun. **180**, 383 (2000).
[7] P. Sprangle, J. R. Penano, and B. Hafizi, Phys. Rev. E **66**, 046418 (2002).
[8] L. Wöste *et al.*, Laser and Optoelectronics **29**, 51 (1997).
[9] J. Kasparian, M. Rodriguez, G. Méjean, J. Yu, E. Salmon, H. Wille, R. Bourayou, S. Frey, Y.-B. André, A. Mysyrowicz, R. Sauerbrey, J.-P. Wolf, and L. Wöste, Science **301**, 61 (2003).
[10] C. P. Hauri, W. Kornelis, F. W. Helbing, A. Heinrich, A. Couairon, A. Mysyrowicz, J. Biegert, and U. Keller, Appl. Phys. B **79**, 673 (2004).
[11] M. Mlejnek, E. M. Wright, and J. V. Moloney, Opt. Lett. **23**, 382 (1998).
[12] S. Tzortzakis, M. Franco, B. Prade, A. Mysyrowicz, A. Couairon, and L. Bergé, Phys. Rev. Lett. **87**, 213902 (2001).
[13] L. Sudrie, A. Couairon, M. Franco, B. Lamouroux, B. Prade, S. Tzortzakis, and A. Mysyrowicz, Phys. Rev. Lett. **89**, 186601 (2002).
[14] V. P. Kandidov, I. S. Golubtsov, and O. G. Kosareva, Quantum Electron. **34**, 348 (2004).
[15] A. Matijosius, J. Trull, P. Di Trapani, A. Dubietis, R. Piskarkas, A. Varanavicius, and A Piskarkas, Opt. Lett. **29**, 1123 (2004).
[16] A. Couairon, S. Tzortzakis, L. Bergé, M. Franco, B. Prade, and A. Mysyrowicz, J. Opt. Soc. Am. B **19**, 1117 (2003).
[17] Multiphoton ionization of free electrons in gases is replaced by multiphoton electron-hole pairs generation in solids.
[18] G. Méchain, A. Couairon, M. Franco, B. Prade, and A. Mysyrowicz, Phys. Rev. Lett. **93**, 035003 (2004).
[19] A. L. Gaeta, Phys. Rev. Lett. **84**, 3582 (2000).
[20] J. Kasparian, R. Sauerbrey, and S. L. Chin, Appl. Phys. B **71**, 877 (2000).
[21] G. Méchain, A. Couairon, Y.-B. André, C. D'Amico, M. Franco, B. Prade, S. Tzortzakis, A. Mysyrowicz, and R. Sauerbrey, Appl. Phys. B **79**, 379 (2004).
[22] G. Fibich, S. Eisenmann, B. Ilan, and A. Zigler, Opt. Lett. **29**, 1772 (2004).
[23] H. Schroeder, J. Liu, and S. L. Chin, Opt. Express **12**, 4768 (2004).
[24] W. Liu, S. L. Chin, O. Kosareva, I. S. Golubtsov, and V. P. Kandidov, Opt. Commun. **225**, 193 (2003).
[25] Z. Wu, H. Jiang, L. Luo, H. Guo, H. Yang, and Q. Gong, Opt. Lett. **27**, 448 (2002).
[26] L. V. Keldysh, Zh. Eksp. Teor. Fiz. **47**, 1945 (1964); [Sov. Phys. JETP **20**, 1307 (1965)].
[27] A.-C. Tien, S. Backus, H. Kapteyn, M. Murnane, and G. Mourou, Phys. Rev. Lett. **82**, 3883 (1999).
[28] L. M. Frantz and J. S. Nodvik, J. Appl. Phys. **34**, 2346 (1963).
[29] K. D. Moll, A. L. Gaeta, and G. Fibich, Phys. Rev. Lett. **90**, 203902 (2003).
[30] F. Wise and P. Di Trapani, Optics & Photonics News **13**, 28 (2002).
[31] T. Brabec, and F. Krausz, Rev. Mod. Phys. **72**, 545 (2000).